Series Elastic Actuator Development for a Biomimetic Walking Robot

David W. Robinson, Jerry E. Pratt, Daniel J. Paluska, and Gill A. Pratt

MIT Leg Laboratory
545 Technology Sq. Rm 006, Cambridge, MA 02139 USA
http://www.ai.mit.edu/projects/leglab/

Abstract— **Series Elastic Actuators have linear springs intentionally placed in series between the motor and actuator output. The spring strain is measured to get an accurate estimate of force. Despite using a transmission to achieve high force/mass and high power/mass, the spring allows for good force control, high force fidelity, minimum impedance, and large dynamic range.**

A second order linear actuator model is broken into two fundamental cases: fixed load – high force (forward transfer function), and free load – zero force (impedance). This model is presented with dimensional analysis and extends previous linear models to include friction. Using the model and dimensionless groups, we examine nonlinear effects of motor saturation as it relates to large force bandwidth and nonlinear friction effects such as stiction. The model also helps to clarify how the springs help and hinder the operation of the actuator.

The information gained from the model helps to create a design procedure for Series Elastic Actuators. Particular emphasis is placed on choosing the spring constant for the elastic element. Large force bandwidth requires a high spring constant. Minimizing nonlinear friction and impedance requires a low spring constant. The design procedure tries to balance these competing requirements and is used to construct a physical actuator.

Keywords— **Series Elastic Actuators, Force Control, Biomimetic Robots**

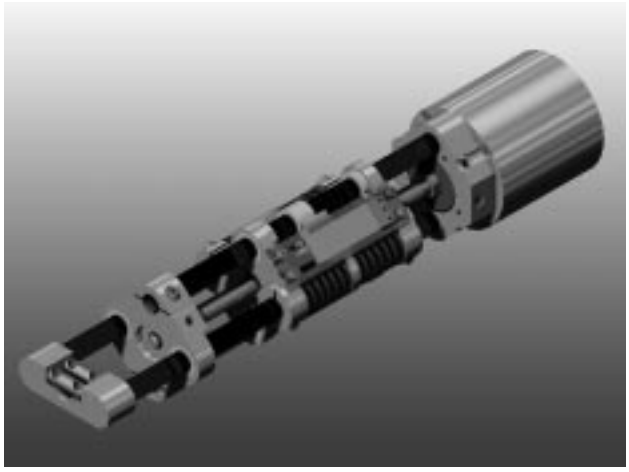

Fig. 1. The prototype actuator has a brushless DC motor rigidly connected to a ballscrew which drives the linear motion. The ballscrew nut is coupled to the output through four die compression springs. The spring compression is measured with a linear potentiometer. The actuator can output over 1350 N and move at 25 cm/second.

I. Introduction

BIOMIMETIC robots, as commonly defined, mimic the structure and movement of humans and animals. Regardless of the current state of the art in robotic motion and force control, there are many things that humans and animals perform better than robots. While much effort has gone into understanding biomimetic robot actions such as walking [1], running [2], catching [3], grasping [4], swimming [5], etc., competence in these areas is still inferior to that of biological counterparts.

Of particular interest in our work is the construction and control of dynamically stable legged robots. Our walking and running robots have three major constraints, and these constraints in turn drive actuator research. These constraints are: 1—The robot must be self supporting. This puts severe limits on the force/mass and power/mass ratio of the actuators. 2—The actuators of the robot must not be damaged during impact steps or falls and must maintain stability in the presence of impacts. 3—The actuators must be force controllable because the algorithms used for robot locomotion are force control based.

In this paper, we explain the design guidelines followed in the construction of an electro-mechanical actuator (figure 1) to be used in a 7-link 12-degree-of-freedom 3D walking biped robot. This actuator, called a *Series Elastic Actuator* [6], has an intentional spring in series with the transmission and the actuator output. The spring somewhat reduces bandwidth, but for our low bandwidth application this is unimportant. In exchange, Series Elastic Actuators are low motion, high force/mass, high power/mass actuators with good force control as well as impact tolerance.

The design guidelines for the actuators come from investigating a second order linear actuator model.

The model is broken into two fundamental cases: fixed load–high force (forward transfer function), and free load–zero force (impedance). These cases help explain the effect of spring constant and controller parameters. The model also extends previous models to include friction and is generalized by use of dimensionless groups. *Rules of Thumb* for designing Series Elastic Actuators are explained and a physical prototype actuator is also described.

II. Related Work

A. Actuators

Many people have used compliant actuators or have studied the control of robots with flexible links or compliant joints [7], [8], [9], [10], [11], [12]. This work has been mostly concerned with mitigating the effect of the compliance rather than taking advantage of it. The highest performance force controlled actuator has been a brushless DC motor rigidly connected to a robot link, also know as direct-drive [13]. These actuators eliminate friction and backlash, typical of motors with transmissions. To compensate for the loss of transmission, direct-drive actuators must be large in order to achieve adequate torque. This means increased motor mass and cost.

Howard introduced the idea of measuring springs in series with an actuator's output by monitoring the displacement between actuator output and motor position, thus inferring spring deflection. [14]. This differential measurement is error prone because there is noise between those two points due to the transmission. Pratt and Williamson [6], [15] developed Series Elastic Actuators by directly measuring the strain of a spring in series with transmission and actuator output. They pointed out that biomimetic actuators can trade off small motion bandwidth for good force control. Also, since the spring deforms a significant amount, the fidelity compared to typical strain gauge structures for force control is much higher.

B. Robots

Several biomimetic robots using Series Elastic Actuators have been constructed and demonstrated. *Spring Turkey* [16] and *SpringFlamingo* [1] use linear drive Series Elastic Actuators and *COG* [17]uses rotary actuators. These robots are all force controlled and use their natural dynamics to perform rhythmic tasks such as walking and turning cranks.

Other laboratories have also worked on walking. The most remarkable being *P2*, an autonomous walking robot constructed by the Honda Research Laboratory [18]. It uses Harmonic Drive Motors for actuation and has visco-elastic material in the joints for shock tolerance, as opposed to our series elastic approach. *P2*'s joints are position controlled with feed forward pattern generation and feedback from 6-axis force-torque sensors in the ankles.

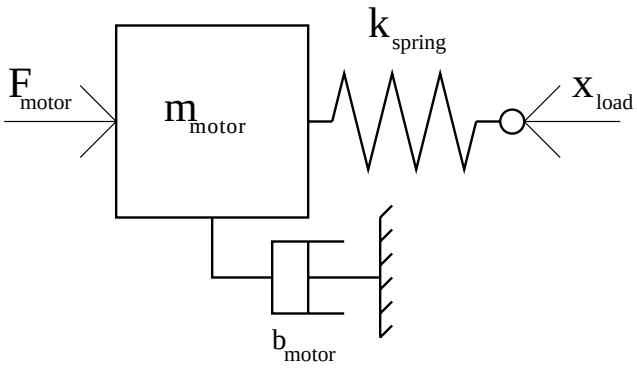

Fig. 2. Mass spring model for the Series Elastic Actuator. The mass has a driving force and viscous friction. The force output of the actuator is determined by the compression of the spring.

III. Actuator Model

A previous paper [6] and thesis [15] investigated Series Elastic Actuators and discussed some details regarding the design of rotary Series Elastic Actuators. In this paper we extend the Series Elastic Actuator model to include friction and describe the model as two fundamental cases using dimensionless groups.

A. Model

The model we use for a Series Elastic Actuator is a second-order lumped mass-spring-damper with a driving force on the mass and a position input from the environment on the spring (figure 2). The perfect force input assumption is justified because the time constant of the motor is significantly faster than our low frequency operating range. The choice of a position constraint on the spring output has been explained by previous authors [19], [20], [21] in terms of admittance/impedance and position causality of the environment.

The lumped mass includes dynamic motor mass and the transmission element masses as seen through the transmission. The motor friction is also seen through the transmission. The spring is the actual spring.

In our analysis we are most interested in the force through the spring which is the force acting on the robot link. This allows us to look at two cases. For the forward transfer functions we assume that the load end is fixed. The other case of interest is at zero force with the load end free. This is the output impedance. The transfer functions for these two cases completely

specify the linear characteristics of the actuator.

The force in the spring, F_l, is a function of two variables: the force input from the motor, F_m, and the relative position of the load, x_l. This relationship is derived to be:

$$F_l(s) = \frac{F_m(s) - (m_m s^2 + b_m s)x_l(s)}{\frac{m_m}{k_s}s^2 + \frac{b_m}{k_s}s + 1}. \qquad (1)$$

Feedback control of the actuator is closed by measuring the deflection of the spring which implies the force output, F_l, of the actuator. We use a unity feedforward term in conjunction with a PD controller on the error with gains K_p and K_d for the proportional and derivative terms respectively. The force to the motor, F_m is determined by

$$F_m = (F_d - F_l)(K_p + K_d s) + F_d \qquad (2)$$

where F_d is the desired force.

Combining equations 1 and 2 yields the closed loop equation for the force through the spring:

$$F_l(s) = \frac{(K_d s + K_p + 1)F_d(s) - (m_m s^2 + b_m s)x_l(s)}{\frac{m_m}{k_s}s^2 + \frac{b_m + k_s K_d}{k_s}s + (K_p + 1)}. \qquad (3)$$

By looking at the different inputs, this equation can be separated into two cases.

B. Case 1: Fixed Load

The transfer function between motor force input and actuator output can be taken from equation 1 and written explicitly as:

$$\frac{F_l(s)}{F_m(s)} = \frac{1}{\frac{m_m}{k_s}s^2 + \frac{b_m}{k_s}s + 1}. \qquad (4)$$

Equation 4 will be referred to as is the open loop transfer function for case one with the load end fixed.

By imposing the fixed end condition again and using equation 3, we can write the closed loop forward transfer function for case one which relates the desired force to the output force:

$$\frac{F_l(s)}{F_d(s)} = \frac{K_d s + (K_p + 1)}{\frac{m_m}{k_s}s^2 + \frac{b_m + k_s K_d}{k_s}s + (K_p + 1)}. \qquad (5)$$

At low frequency, this transfer function is equal to unity, and in the limit at high frequency it goes to zero.

C. Case 2: Free end with zero force

To see the zero load impedance, case two, we write:

$$\frac{F_l(s)}{x_l(s)} = \frac{-(m_m s^2 + b_m s)}{\frac{m_m}{k_s}s^2 + \frac{b_m + k_s K_d}{k_s}s + (K_p + 1)}. \qquad (6)$$

Opposite of the closed loop forward transfer function, the impedance at low frequency is idealiy equal to zero. At high frequency, it is equal to k_s, the spring constant of the physical spring. This will be dicussed later.

D. Dimensionless formulation

Both the open and closed loop transfer functions, equation 4 and equation 5, and the output impedance, equation 6, can be written in dimensionless form.

First, notice that there are two natural frequencies. The first is the natural resonance of the motor mass and spring ω_n. The second is the controlled natural frequency ω_c.

$$\omega_n = \sqrt{\frac{k_s}{m_m}} \qquad \omega_c = \sqrt{\frac{k_s(K_p + 1)}{m_m}} \qquad (7)$$

Using these two natural frequencies and the following dimensionless groups we can non-dimensionalize both the open and closed loop equations equations of case one and the impedance of case two.

$$\begin{aligned} S &= \frac{s}{\omega_n} \\ \Omega &= \frac{\omega_c}{\omega_n} = \sqrt{K_p + 1} \\ B &= \frac{b_m}{k_s}\omega_n \\ \Gamma &= K_d \omega_n \end{aligned} \qquad (8)$$

- S normalizes the equation to the natural resonance of the motor mass spring system of the actuator.
- Ω is a measure of the increase in bandwidth due to the controller. Ω is always ≥ 1.
- B is a scaled natural damping term physically present in the construction of the actuator.
- Γ represents the scaled controller damping gain.

The dimensionless open loop, closed loop, and output impedance transfer functions are:

$$G_{ol}(S) = \frac{F_l(S)}{F_m(S)} = \frac{1}{S^2 + BS + 1} \qquad (9)$$

$$G_{cl}(S) = \frac{F_l(S)}{F_d(S)} = \frac{\Gamma S + \Omega^2}{S^2 + (\Gamma + B)S + \Omega^2} \qquad (10)$$

$$Z_{cl}(S) = \frac{F_l(S)}{k_s x_l(S)} = \frac{-S(S + B)}{S^2 + (\Gamma + B)S + \Omega^2} \qquad (11)$$

These models are the basis for the analysis in the rest of the paper.

IV. Model Analysis

In this section, we examine motor saturation, large force bandwidth, and friction using the open loop model of case one. Using the closed loop model, we explain the choice of control parameters. Also, we look at nonlinear friction reduction and output impedance due to the controller. These each help understand design tradeoffs that must be made in the actuators, particularly with the choice of spring constant in the elastic element.

A. Saturation, Friction, and Large Force Bandwidth

In order to better understand the effects of force and velocity saturation, we introduce a simple motor saturation model:

$$|F_m| \leq \begin{cases} F_{sat}(1 - \frac{|V_m|}{V_{sat}}) & : \quad |V_m| \leq V_{sat} \\ 0 & : \quad |V_m| > V_{sat} \end{cases} \tag{12}$$

where F_{sat} and V_{sat} are the maximum force and maximum velocity respectively for the motor. V_m is the actual motor velocity.

When the motor is not pegged at saturation conditions, it still follows a linear back-EMF model where:

$$F_{emf} = \frac{F_{sat}}{V_{sat}} V_m. \tag{13}$$

The back-EMF can be thought of as an equivalent damping because it relates a loss in motor force due to motor velocity just like the term b_m. The equivalent damping coefficient for the back EMF is F_{sat}/V_{sat}. We then modify our B group to be

$$B = \frac{b_m + \frac{F_{sat}}{V_{sat}}}{k_s} \omega_n. \tag{14}$$

The B group plays an important role in the large force bandwidth. Also, by incorporating the velocity saturation as an equivalent force we can investigate large force bandwidth in terms of the saturation force only.

Large force bandwidth is independent of the control system and is only a function of the open loop dynamics of the system, equation 9. We can write the magnitude function of equation 9 in terms of a normalized frequency, $W = \omega/\omega_n$:

$$Mag = \frac{F_l}{F_m} = \frac{1}{\sqrt{(1 - W^2)^2 + (BW)^2}} \tag{15}$$

While the magnitude equation relates the load force F_l as a function of the motor force F_m in the linear range, it can also relate maximum load force output, $F_{l_{max}}$, as a function of the maximum motor output, F_{sat}.

$$\frac{F_{l_{max}}}{F_{sat}} = \frac{1}{\sqrt{(1 - W^2)^2 + (BW)^2}}. \tag{16}$$

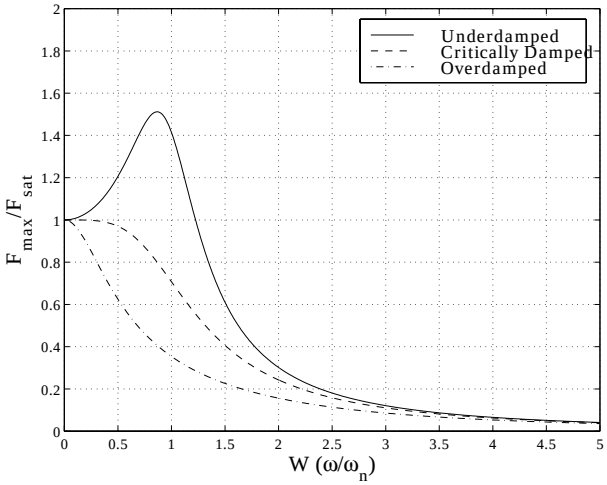

Fig. 3. The B group (generalized damping) defines the large force bandwidth of the actuator. The three lines represent underdamped, critically damped, and overdamped frequency response.

Figure 3 shows different values for B with respect to the maximum available force output due to force saturation. There are two points of particular interest: frequencies around ω_n and the high frequencies. The damping affects how well the system handles large forces near the natural frequency. With an overdamped system, the available force amplitude at resonance dramatically reduces the available force amplitude. But also for an underdamped system, the components must be able to withstand possible overload conditions. Regardless of the damping in the system, high amplitude forces at high frequency are impossible. This is because the motor is fighting the effects of the spring at those frequencies.

This analysis confirms previous work stating that elasticity in an actuator reduces large force bandwidth and increases control effort at high frequencies [6], [14]. Therefore, increasing k_s will increase bandwidth. But, from the constraints of friction and saturation, we need to choose a minimum acceptable large force bandwidth. This operational frequency, ω_o, will define the lower bound for the spring constant, k_s.

The shape of the large force bandwidth is solely a function of the dimensionless group B. In standard control textbooks [22], the resonance for second order systems is defined by the magnitude of ζ_n, the damping

ratio. Since the natural frequency has been normalized to one for the open loop transfer function, ζ_n is related to B by:

$$\zeta_n = \frac{B}{2}. \tag{17}$$

Therefore, we can talk about B in terms of under, critical, and over damping as the three curves in figure 3 show.

Let us now take a closer look at B.

$$\begin{aligned} B &= \frac{b_m + \frac{F_{sat}}{V_{sat}}}{k_s}\omega_n \\ &= \frac{b_m + \frac{F_{sat}}{V_{sat}}}{k_s}\sqrt{\frac{k_s}{m_m}} \\ &= \left(b_m + \frac{F_{sat}}{V_{sat}}\right)\sqrt{\frac{1}{k_s m_m}} \end{aligned} \tag{18}$$

Equation 18 helps us see the relationship of B to the physical model parameters. In general, we want B to be as small as possible to increase bandwidth. Equation 18 can help define design guidelines regarding friction.

- b_m — Make the actuator with as little drive friction as possible.
- $\frac{F_{sat}}{V_{sat}}$ — Minimize back EMF.
- m_m — Using a larger motor mass will decrease resonant frequency thus making the apparent damping smaller.
- k_s — A larger spring constant decreases spring deflection. Spring and motor velocity subsequently decrease and therefore damping decreases.

It is also important to remember that both b_m and m_m as represented in this model are seen through a transmission reduction and are scaled by N^2, where N is the reduction. Therefore a decrease in reduction will decrease the damping.

B. Controller Gains

Up to this point in the analysis we have only worked with the open loop forward transfer function. From here, we will be dealing with the closed loop behavior and therefore should briefly mention selection of controller gains.

Using the closed-loop characteristic equation (denominator of equation 10 and 11) in conjunction with the dimensionless groups (equation 8), the controller gain values for a PD controller with unity feed forward can be explicitly defined to get a desired closed loop natural frequency w_c and damping ratio ζ_c.

The proportional gain is found from the definition of Ω.

$$\Omega^2 = K_p + 1$$

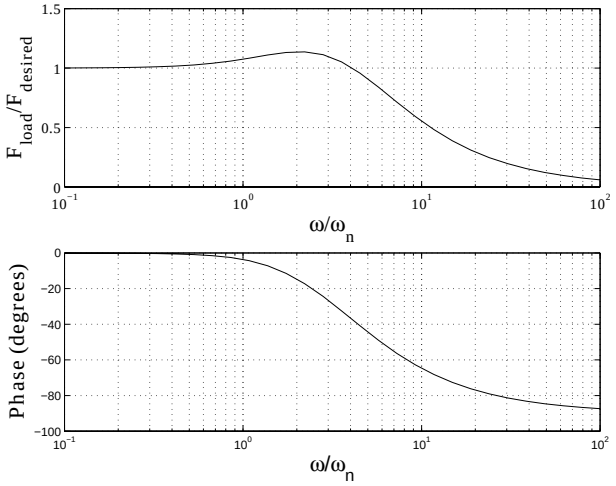

Fig. 4. This is a bode plot of the closed loop system. $\Omega = 3$ and $\zeta_c = 1$.

$$\Longrightarrow K_p = \frac{w_c^2}{w_n^2} - 1 \tag{19}$$

The derivative gain is found from the damping term of the characteristic equation.

$$\begin{aligned} 2\zeta_c\Omega &= B + \Gamma \\ \Longrightarrow K_d &= \frac{2\zeta_c\omega_c m_m - b_m}{k_s} \end{aligned} \tag{20}$$

As an example figure 4, shows a bode plot of the closed loop forward transfer function: $\Omega = 3$ and $\zeta_c = 1$.

C. Stiction

Coulomb friction and stiction are dramatically affected by the introduction of the spring into the actuator. A form of this analysis was originally documented in [23] and is included for completeness. Because of stiction, the lumped mass will not move until

$$F_m - F_l = F_m - F_d + F_e = F_s \tag{21}$$

where F_e is the feedback force error and F_s is the force due to stiction. Since, stiction is a low frequency phenomenon, we assume that the derivative term of the controller is negligible. The force to the motor due to the error then becomes

$$F_m \approx K_p F_e + F_d. \tag{22}$$

Using equations 21 and 22 we can solve for the force error F_e.

$$F_e \approx \frac{1}{K_p + 1} F_s \tag{23}$$

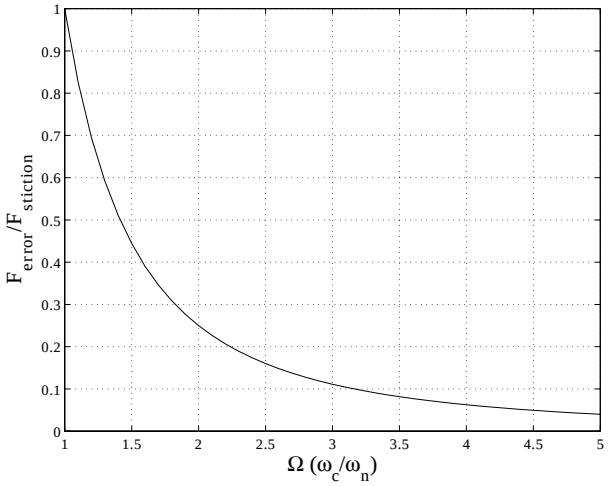

Fig. 5. There is a parabolic relationship of the force error due to stiction force in the motor which a function of spring stiffness and proportional controller gain. As Ω increases non-linear friction forces are dramatically decreased.

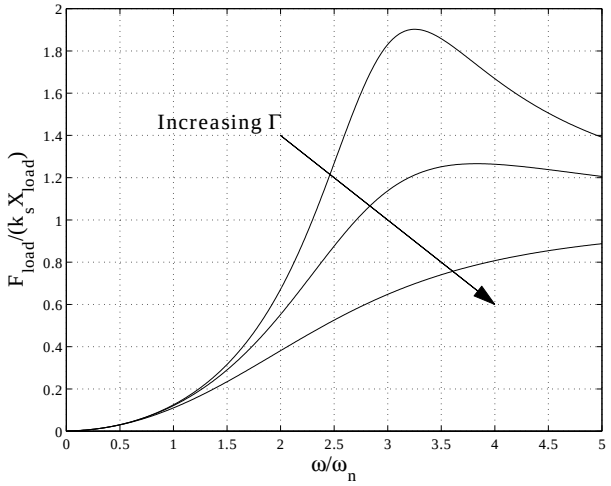

Fig. 6. The impedance of the actuator at low frequency is zero and is k_s at high frequency. In this example $\Omega = 3$. As Γ is increases there is an effective reduction in the impedance at the controlled natural frequency.

This shows that the force error due to stiction is related by the dimensionless group Ω.

$$F_e \approx \frac{1}{\Omega^2} F_s \tag{24}$$

Remember that Ω is the ratio between the resonant frequency of the mass-spring system and the controlled natural frequency. Increasing Ω reduces the effect of stiction. So, there are two ways to effectively reduce stiction: 1–increase ω_c by increasing the gain or 2–decrease ω_n by reducing the spring constant. The relationship is inverse parabolic and can be visualized in figure 5. Theoretically, to eliminate stiction we should have as soft a spring as possible. However, part of the design is to evaluate an acceptable level of stiction reduction.

As an example, if the controller gain is turned off, $K_p = 0$, then $\omega_c = \omega_n \Rightarrow \Omega = 1$. As the gain is increased, there is a rapid decrease in the noticeable stiction force in the system. If we set our controlled natural frequency three times greater than the mass-spring resonance, then stiction is reduced to 11% of its original value.

D. Impedance

Equation 11 shows the dimensionless form of output impedance. At low frequencies the impedance is zero but as frequency increases, in the limit the impedance is equal to the spring constant, k_s. Equation 11 normalizes to k_s and figure 6 shows an example of the impedance for different values of Γ which represents the derivative gain. In this example, the impedance around the actuator natural frequency, ω_n, is significantly reduced to an equivalent range regardless of Γ.

There are three ways to decrease the output impedance for Series Elastic Actuators.

- Increase the control gain. This drives the impedance resonance further away from the operational bandwidth.
- Decrease the spring constant. This contributes a reduction in impedance in two ways. It effectively increases Ω and linearly scales the impedance profile.
- Increase the derivate gain. As seen in figure 6, Γ's major contribution is to reduce impedance resonance at the controlled natural frequency.

The most important of the above three is the spring constant. For low impedance we want k_s to be as low as possible. Just as in stiction reduction, we need to define a maximum allowable k_s, so that we can balance a desire for low impedance and large force bandwidth.

V. Physical Actuator

The theoretical work just presented has a practical side too. The following discussion elaborates on decisions made during the design and construction of an actuator (figure 1) for a biomimetic walking robot.

A. Component Selection

The design space for Series Elastic Actuators is very large. Besides geometry and topology there are five major components: motor, transmission, spring, sensor, and controller. Of all five components, choosing

the spring is the only part of the actuator which requires unique perspective and is discussed in the next section.

The specifications for the motor and transmission need to be done based on the force, speed, and power requirements for a given task. These design requirements are not unique to Series Elastic Actuators and would be done for any actuator.

As a helpful aid to the final operation, the motor and transmission should be selected with the idea of keeping friction and motor saturation low. Motor friction b_m which is seen through the transmission N^2, is kept at a minimum in the prototype actuator by using a brushless DC motor. The actuator also reduces drive friction by designing the center of mass, center of friction, and center of stiffness to be colinear along the ball screw axis [24].

Transmission dynamics should also be kept to a minimum as it is one of two limiting factors in using high feedback gain [25], [23]. We used a frameless motor configuration where the motor magnets are mounted directly onto an extended ballscrew shaft instead of using a coupling, gears, or a belt drive.

The other limiting component to achieve high feedback gain is the sensor. The sensor needs to directly measure the spring deflection. This insures that the feedback measurement is a representation of true force. Noise in the sensor is also very detrimental to operation. We use a linear potentiometer to measure spring deflection.

B. Choosing the Spring Constant

Selecting the spring constant is a balance between large force bandwidth needing a high k_s and stiction and impedance needing a low one. We present some guidelines for choosing a spring constant.

1. Select a motor and transmission based on the force, speed, and power requirements for the given task. This will define the lumped motor mass, damping, and saturation characteristics seen through the reduction.
2. Define an operational bandwidth, ω_o, for which the actuator will need large forces. In other words, define a required large force bandwidth profile (section IV-A). This profile is independent of controller and depends solely on ω_n and B. This places a lower bound on k_s. Most likely, the operational bandwidth may be a little greater than but close to the selected natural frequency.
3. Stiction (section IV-C) and Impedance (section IV-D) place an upper bound on k_s. This is a function of the controller values Ω and Γ. Insure that the controller gains can be raised to acceptable levels of stiction and impedance reduction.

TABLE I
PHYSICAL PROPERTIES OF PROTOTYPE ACTUATOR

Parameter	Value	Units
Max Force	1350	N
Cont. Force	750	N
Min Force	2.5	N
Max Speed	.25	m/s
Mass	1.13	kg
Dynamic Mass	128	kg
Spring Constant	315	kN/m
ω_n	7.9	Hz
ω_c	35	Hz
ζ_n	0.2	no units
Ω	4	no units
B	0.1	no units

4. It may be necessary to iterate. The non-dimensional equations will help to guide to know whether to increase or decrease k_s and how much effect it will have.

C. Physical Actuator Characteristics

The requirements for the actuator came from a physically realistic simulation of a 12 degree-of-freedom 3D walking robot. We estimated a weight distribution for the robot assuming that two actuators would be located in each shin and thigh. Four more actuators would be located in the body along with the majority of the electronics. A common actuator (figure 1) that satisfies the requirements for each of the joints in the simulation was designed and built using the guidelines described in this paper. Table I shows the physical characteristics of the actuator.

The actuator has a large dynamic range. The minimum resolvable force is 2.5 N and it can output over 1350 N which gives a dynamic range over 500. Considering the actuator has 2mm/rev reduction in the ball screw, the dynamic range is impressive [26]. Although, Series Elastic Actuators may not have as large a dynamic range as comparable direct drive actuators, the weight savings are well worth the tradeoff for our intended weight sensitive application.

VI. CONCLUSIONS AND FUTURE WORK

We use a second order model of a Series Elastic Actuator to investigate the open and closed loop forward transfer function and the impedance of the system. These two cases completely describe the linear characteristics of the actuator. The model includes friction and motor saturation and is generalized by using dimensional analysis. We examine large force bandwidth, controller gains, and minimizing the effects of

stiction.

The model has helped to create design guidelines for Series Elastic Actuators. Emphasis is placed on choosing the spring constant of the elastic element. Large force bandwidth requires a high spring constant. Minimizing nonlinear friction and impedance requires a low spring constant. The choice of spring constant has been shown to be a compromise between these competing requirements.

A physical actuator designed and constructed with the guidelines from this paper has been build and will be used in a 7-link 12 degree-of-freedom walking robot.

In both the analysis and physical actuator, we use a linear spring. Future work will investigate nonlinear stiffening springs which may ease the design tradeoffs currently required.

References

[1] Jerry Pratt and Gill Pratt, "Intuitive control of a planar bipedal walking robot," *IROS'98*, 1998.

[2] Marc. H. Raibert., *Legged Robots That Balance.*, MIT Press, Cambridge, MA., 1986.

[3] Won Hong, "Robotic catching and manipulatoin using active vision," M.S. thesis, Massachusetts Institute of Technology, September 1995, Mechical Engineering.

[4] J. Kenneth Salisbury and Mandayam A. Srinivasan, *Proceedings of The First PHANToM User's Group Workshop*, MIT AI Laboratory, Cambridge, MA., 1996, September 27-30, 1996.

[5] M.S. Triantafyllou and G.S. Triantafyllou, "An efficient swimming machine," *Scientific American*, vol. 272, no. 3, pp. 64–70, March 1995.

[6] Gill A. Pratt and Matthew M. Williamson, "Series elastic actuators," *IEEE International Conference on Intelligent Robots and Systems*, vol. 1, pp. 399–406, 1995.

[7] H. Hanafusa and H. Asada, "A robotic hand with elastic fingers and its application to assembly process," *IFAC Symposium on Information and Control Problems in manufacturing Technology*, pp. 127–138, 1977, Tokyo.

[8] Matthew Mason, "Compliant motion," in *Robot Motion: Planning and Control*. 1982, pp. 305–322, MIT Press.

[9] Robert H. Cannon Jr. and Eric Schmitz, "Initial experiments on the end-point control of a flexible one-link robot.," *International Journal of Robotics Research*, vol. 3, no. 3, pp. 62–75, 1984.

[10] Mark W. Spong, "Modeling and control of elastic joint robots," *Journal of Dynamic Systems, Measurement, and Control*, vol. 109, pp. 310–319, Dec. 1987.

[11] S. Sugano, S. Tsuto, and I. Kato, "Force control of the robot finger joint equipped with mechanical compliance adjuster," *International Conference on Intelligent Robots and Systems*, pp. 2005–2012, 1992.

[12] Dieter Vischer and Oussama Khatib, "Design and development of high-performance torque-controlled joints," *IEEE Transactions on Robotics and Automation*, vol. 11, no. 4, pp. 537–544, 1995.

[13] H. Asada and K. Youcef-Toumi, *Direct Drive Robots: Theory and Practice*, MIT Press, Cambridge, MA, 1987.

[14] Russel D. Howard, *Joint and Actuator Design for Enhanced Stability in Robotic Force Control*, Ph.D. thesis, Massachusetts Institute of Technology, September 1990.

[15] Matthew M. Williamson, "Series elastic actuators," M.S. thesis, Massachusetts Institute of Technology, June 1995.

[16] Jerry E. Pratt, "Virtual model control of a biped walking robot," M.S. thesis, Massachusetts Institute of Technology, May 1995.

[17] Rodney A. Brooks, Cynthia Breazeal, Matthew Marjanovic, Brian Scassellati, and Matthew Williamson, *The Cog Project: Building a Humanoid Robot*, Springer-Verlag, 1999, To appear in a Springer-Verlag Lecture Notes in Computer Science Volume.

[18] Kazuo Hirai, Masato Hirose, Yuji Haikawa, and Toru Takenaka, "The development of honda humanoid robot," *International Conference on Robotics and Automation*, 1998.

[19] N. Hogan, "Impeadance control: An approach to manipulation: Part i - theory, part ii - implementation, part iii - applications," *J. of Dynamic Systems, Measurement and Control*, vol. 107, pp. 1–24, 1985.

[20] S.C. Jacobsen, C.C. Smith, K.B. Biggers, and E.K. Iverson, "Behavior based design of robot effectors," *Proc. of the Fourth Int'l Symp. on robotics research*, pp. 41–55, 1989.

[21] C.C. Smith, S.C. Jacobsen, L.A. Robins, D.W. Wilcox, and S.J. Bohn, "Design and control of electromechanical actuation systems," *ASME DSC Modelling and Control of Compliant and Rigid Motion Systems Winter Annual Meeting*, pp. 137–144, 1991, Dec 1-6.

[22] Katsuhiko Ogata, *Modern Control Engineering*, Prentice Hall, 1990.

[23] Jerry E. Pratt, "Effects of spring constant on series elastic actuator stability, dynamic range, and large force bandwidth," Unpublished Project Report for MIT's Modeling and Simulation of Dynamic Systems Class (2.141), 1996.

[24] Alexander H. Slocum, *Precision Machine Design*, Prentice-Hall, 1992.

[25] S.D. Eppinger and W.P. Seering, "Understanding bandwidth limitations in robot force control," *IEEE Int'l Conf' on Robotics and Automation*, vol. 2, pp. 904–909, 1987, Raleigh, NC.

[26] John Hollerbach, Ian Hunter, and John Ballantyne, "A comparative analysis of actuator technologies for robotics," in *Robotics Review 2*. 1991, pp. 299–342, MIT Press.